

Design and analysis of digital materials for physical 3D voxel printing

Jonathan Hiller and Hod Lipson

Cornell Computational Synthesis Lab, Cornell University, Ithaca, New York, USA

Abstract

Purpose – Virtual voxels (3D pixels) have traditionally been used as a graphical data structure for representing 3D geometry. The purpose of this paper is to study the use of pre-existing physical voxels as a material building-block for layered manufacturing and present the theoretical underpinnings for a fundamentally new massively parallel additive fabrication process in which 3D matter is digital. The paper also seeks to explore the unique possibilities enabled by this paradigm.

Design/methodology/approach – Digital RP is a process whereby a physical 3D object is made of many digital units (voxels) arranged selectively in a 3D lattice, as opposed to analog (continuous) material commonly used in conventional rapid prototyping. The paper draws from fundamentals of 3D space-filling shapes, large-scale numerical simulation, and a survey of modern technology to reach conclusions on the feasibility of a fabricator for digital matter.

Findings – Design criteria and appropriate 3D voxel geometries are presented that self-align and are suitable for rapid parallel assembly and economical manufacturing. Theory and numerical simulation predict dimensional accuracy to scale favorably as the number of voxels increases. Current technology will enable rapid parallel assembly of billions of microscale voxels.

Research limitations/implications – Many novel voxel functions could be realized in the electromechanical and microfluidic domains, enabling inexpensive prototyping of complex 3D integrated systems. The paper demonstrates the feasibility of a 3D digital fabricator, but an instantiation is out of scope and left to future work.

Practical implications – Digital manufacturing offers the possibility of desktop fabrication of perfectly repeatable, precise, multi-material objects with microscale accuracy.

Originality/value – The paper constitutes a comprehensive review of physical voxel-based manufacturing and presents the groundwork for an emerging new field of additive manufacturing.

Keywords Manufacturing systems, Rapid prototypes

Paper type Research paper

Introduction

The transition from analog to digital technologies has revolutionized many fields over the past century – most notably communication and computation – and can be used to similarly revolutionize current rapid prototyping technology. Digital principles allow for perfect replication and zero noise despite using a noisy and inaccurate substrate. Though digital controllers govern the majority of rapid prototyping technologies today, the fabrication processes themselves are still inherently analog: material can be added or removed anywhere, and every dimension has a non-zero error. Consequently, an analog fabrication system cannot make a part more accurate than its own positioning system, and performance degradation is inevitable in every subsequent replication. In contrast, many biological “fabrication” processes exploit digital assembly of fundamental building blocks (DNA, proteins, etc.), which repeatedly assemble into

precise structures despite a very noisy environment and are able to reproduce without loss of accuracy over millions of generations. These principles extend to mechanical replication processes inspired by these biological processes (Zykov *et al.*, 2005), and may have profound implication to additive freeform fabrication as well.

This paper explores a fundamentally new 3D freeform fabrication process exploiting massively-parallel assembly of microscale units. In comparison to traditional (analog) 3D printing in which material is deposited or solidified in an inherent continuum, digital 3D printing imposes finite resolution: the size of a single unit. Advantages of this 3D digital domain include high dimensional accuracy, perfect repeatability, and the inherent capability of low-temperature co-fabrication using a rich and diverse set of materials. These physical, self-aligning, fundamental units are hereafter referred to as “voxels” (3D pixels). Unlike traditional virtual voxels used extensively in computer graphics and computational geometry, here we refer to physical voxels to be used in fabrication. We provide the theoretical background demonstrating that 3D digital printing is a viable freeform fabrication process with unique advantages, and we address

The current issue and full text archive of this journal is available at www.emeraldinsight.com/1355-2546.htm



Rapid Prototyping Journal
15/2 (2009) 137–149
© Emerald Group Publishing Limited [ISSN 1355-2546]
[DOI 10.1108/13552540910943441]

Received: 22 April 2008
Revised: 27 August 2008
Accepted: 6 November 2008

a number of design challenges relating to voxel topology and geometry.

We define the following terms for the purpose of this paper:

- *Voxel*. A fundamental, physical, aligned object, constrained to a repeating unit of physical 3D space. Not necessarily cubic or space filling.
- *Digital material*. Material composed of many such assembled voxels. Refers to the overall material, which is defined by the voxel topology, how the voxels are assembled, and the material each voxel is constructed of.
- *Digital fabricator*. A 3D printer that assembles digital materials – a voxel printer. Note that although most conventional 3D printers use digital control and feedback systems, they are not capable of printing with physical voxels.

Conventional 3D printing, stereo lithography and SLS technologies can fabricate 3D parts of varying precision, but typically of a single, homogeneous material (Kaddekar *et al.*, 2004; Zhang *et al.*, 1999; Chua *et al.*, 1998). Current fused deposition modeling technology is capable of producing objects composed of multiple materials, but is limited in precision and is limited to extrudable materials (Malone and Lipson, 2006; Malone *et al.*, 2004). Inkjet fabrication using multiple materials has also been explored (Calvert, 2001) but places even more severe restrictions on the rheological properties of the deposited materials. Digital materials offer the possibility to circumnavigate these challenges as will be described below.

As a fundamentally different approach to 3D printing, Gershenfeld (2005) recently proposed that thinking of fabrication as a digital (voxel based) rather than a continuous process can address these challenges. Although much work has been done in the area of voxels as data structures for computer graphics and CAD (Jense, 1989) and in RP specifically (Chandru *et al.*, 1995; Ma *et al.*, 2001a,b; Lin and Seah, 1998; Lin *et al.*, 2007), here we address the challenges of creating a functional physical voxel printer. The challenges and research associated with this are fundamentally different from the challenges and research-taking place in the field of voxels as data structures. Arbitrary-geometry (programmable) digital fabrication can take place as a top-down approach (Popescu *et al.*, 2006b) or as a bottom-up approach (Tolley *et al.*, 2006). In bottom-up manufacturing, sub-components arrange themselves into a more complex assembly. In top-down manufacturing, an external fabricator directs assembly. Here, we focus on the top-down approach as proposed by Popescu *et al.* (2006a) (Figure 1).

Background

Matter is fundamentally digital if it considered in terms of distinct, regularly repeating regions (voxels) that tessellate 3D space. In much the same way as a digital byte is binary, the occupation of each voxel-space within the solid must be defined as either present or not present. This is captured in the octree representation of a 3D solid (Meagher, 1982), with a constant minimum size of subdivision. Many of the advantages inherent to the digital domain translate into useful mechanical traits. These key advantages are listed as follows:

- *Accuracy*. By geometric design, the voxels will self-align upon assembly so a fabricator need only place the voxel within a certain distance of its final position. Thus,

the precision of the final part depends only on the tolerances of the voxels. This is analogous to a child with 1 mm hand placement precision assembling LEGO™ structures with 5 μm precision. This results in an object more precise than the fabricator that created it.

- *Perfect repeatability*. Digital parts are perfectly repeatable with no loss of 3D information over subsequent replications.
- *Error scaling*. Assuming a large number of voxels compose the finished part, the overall precision of the part scales favorably as random errors of individual voxels tend to cancel out.
- *Multiple materials*. Since each voxel type is pre-manufactured independently, multiple materials may be combined in a single fabrication batch. It is possible to combine materials such as high-melting point metals and low-melting point polymers whose initial processing properties are mutually incompatible. This intrinsic advantage has been noted in the realm of voxel data structures, as well (Chua *et al.*, 2003).
- *Smart voxels*. Prefabricated voxels can also be pre-loaded with simple active components such as transistors, photovoltaics, microvalves, and other sensors and actuators, thereby opening the door to fabrication of complex, functional integrated systems.

Disadvantages to digital manufacturing are analogous to the disadvantages of other digital technologies. Key disadvantages are:

- A finite resolution leads to a loss of generality in the shape that can be fabricated. However, the resolution (voxel size) of digital materials may be chosen to fulfill the desired functionality, in the same way as the bit-rate of digital music or the pixel count of digital pictures is arbitrarily chosen.
- Increased processing complexity. Digital processing of material requires bit-by-bit addressing and therefore more complex machinery and slower processing time. This is again similar to digital signal processing that is generally more complex and significantly slower than analog signal processing.

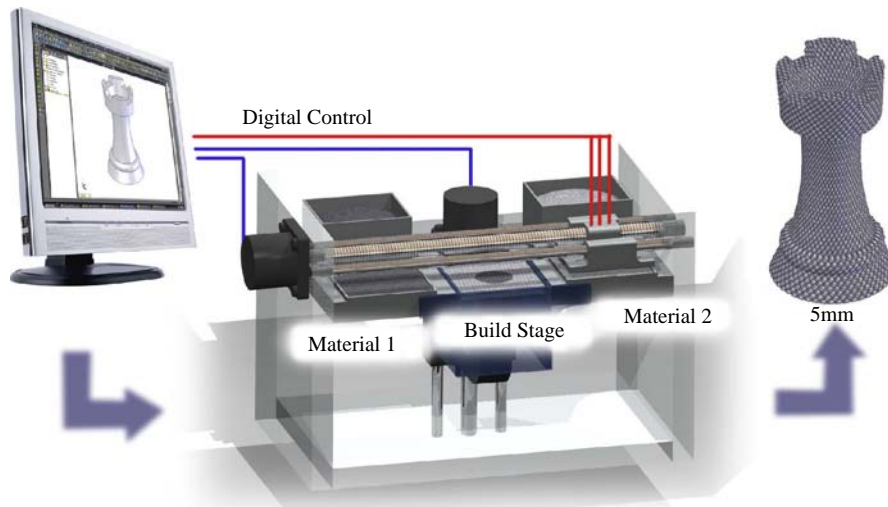
Design of digital materials

In order to fabricate useful, robust devices in a massively parallel assembly operation, the voxels used in digital materials should maximize the following properties. Only the first property is strictly required, whereas the other properties are generally desirable:

- Passively self-align in R^3 relative to neighbors.
- Be invariant to rotation and flip, allowing easier manipulation.
- Rigidly connect to neighbors to maintain strength of final structure.
- Fully tessellate R^3 to allow for fabrication of both dense and sparse solids.
- Be cost-effective to manufacture in large quantities.

Each voxel must be capable of passive self-alignment in R^3 relative to the voxels around it once placed within a certain range. In order to facilitate robust large-scale assembly, the voxel geometry should also be rotation and flip invariant, since active control to align voxels would require prohibitive cost and complexity. Voxels must be rigidly held together, either by geometric interlocking or by post-processing the

Figure 1 The principle of a digital manufacturing process, using spherical voxels



finished assembly. Additionally, it is desirable for the most demanding structural applications that the voxels fully tessellate 3D space such that voids are minimized. Artists such as M.C. Escher have explored many freeform 2D tessellating shapes (Escher, 1971). In 3D, there are two main classes of voxel geometries that fulfill the noted requirements: 2.5D and 3D shapes. In this context, 2.5D voxels can be decomposed into a small number of extruded 2D layers, have 2D rotational symmetry with flip invariance, and interlock only with the layers above and below. 3D voxels incorporate more complex shapes with 3D rotational symmetry that interlocks with voxels on all sides. However, non-space-filling designs may be desirable in applications where weight must be considered. Although largely a subset of the space-filling designs, this category will be considered as well.

Spherical and unique non-space-filling designs are considered separately. There is a general tradeoff between the complexity of the voxel geometry and the complexity of the assembly process.

2.5D voxels

There are two basic shapes that fully tessellate R^2 : the equilateral triangle and the rectangle. Combining two equilateral triangles yields a diamond and three diamonds creates a hexagon. Many other irregular 2D tessellating shapes exist, such as those found in the art of M.C. Escher, but are not considered due to the lack of rotational symmetry, which makes passive alignment difficult. Since the 2.5D voxels interlock only with the layers above and below, each layer must be offset and no interlocking geometry is needed in-plane (Figure 2).

Although 2.5D voxels only interlock in the vertical direction, once two layers are in place they form a rigid structure with positive constraint in the lateral directions. This allows the digital material to be stressed in tension in two directions and compression in all three. Additionally, since the individual voxels can be fabricated with three stacked and bonded layers, conventional multilayer photolithography (Yao *et al.*, 2004) or other layer-bonding techniques can be used to make large numbers of microscale voxels in a batch process. The lack of in-layer interlocking allows an entire layer

of voxels to be passively aligned and selectively placed at once, which is parallel in 2D. However, diamonds can tessellate R^2 in two unique ways, and the hexagonal design has only 3° of rotational symmetry out of six possible orientations, both of which may lead to problems with passive alignment.

3D voxels

There are three distinct topologies that fully tessellate R^3 and can physically interlock with no loss of possible orientations. These are the rectangular prism, a truncated tetrahedron and a truncated octahedron (Figure 3). Other more complex R^3 tessellating solids, such as the rhombic dodecahedron exist, but are not considered here. The rectangular prism is by far the most familiar, and the cube will be considered as the most general case. Neither tetrahedrons nor octahedrons completely tessellate R^3 , but unique truncations of the corners yield this desired property, albeit with rather complex and unfamiliar shapes. In all three cases, the geometry can be designed to physically interlock into a rigid structure with no loss of possible orientations.

Voxels with 3D rotational symmetry interlock in 3D and thus have greater alignment redundancy. However, there are several aspects which make them impractical for large-scale digital manufacturing processes. First, by the very nature of interlocking in 3D, they must be actively assembled in all 3D, which would be a challenging automated process compared to the 1D of active assembly for the 2.5D voxels. Additionally, there is no effective way to manufacture large numbers of these voxels at the microscale with the necessary tolerances.

Non-space-filling voxels

In some applications, it is advantageous to use sparse materials. For instance, when weight or density is critical, greater compliance is needed, or fluids/gasses must penetrate the structure. One solution is to place sacrificial voxels in a regular pattern throughout a structure, which are later removed. If the lattice is too dense to allow efficient removal of the support material, leaving voxel voids during the fabrication process is compatible with all the geometries presented here, so long as they border a sufficient number of realized voxels.

Figure 2 Interlocking, self-aligning 2.5D voxel suitable for digital materials. Thumb tacks are shown for scale

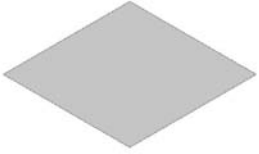
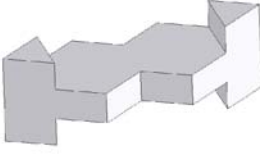
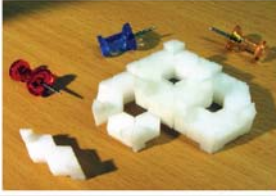
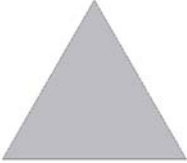
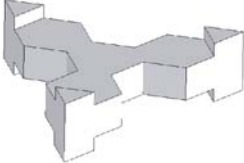


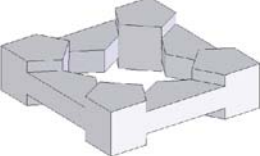


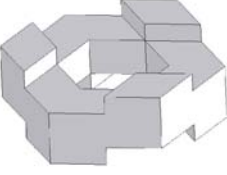

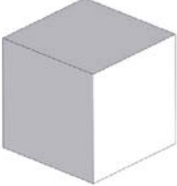
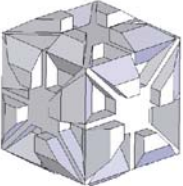
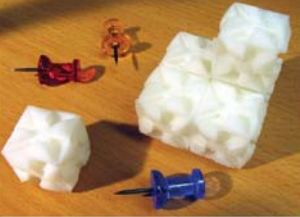
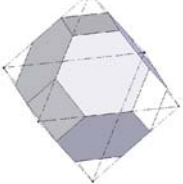
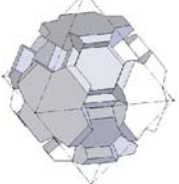
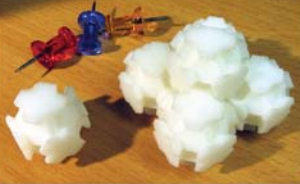
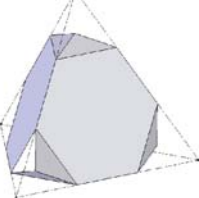
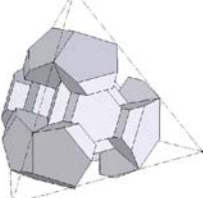

Basic Shape	Interlocking Geometry	Assembled Material
		
		
		
		

Figure 3 Interlocking, space-filling 3D voxel suitable for digital materials. Thumb tacks are shown for scale

Basic Shape	Interlocking Geometry	Assembled Material
		
		
		

Another technique to create sparse digital materials is to remove non-critical material from the 2.5D and 3D voxels. Thus, voids can be selectively introduced while preserving the geometric interlocking properties. This could be carried out such that the voids are isolated (analogous to closed-cell foam), or interconnected to allow fluid flow in specific directions (Mullen *et al.*, 2008). This opens up possibilities in the area of tissue engineering, where factors such as pore size and mechanical properties must be carefully controlled (Yang, 2001; Hollister, 2005).

Spherical voxels

Although close-packed spheres do not fill R^3 , they occupy a majority (74 percent by volume). Spheres also have other practical advantages, which cannot be ignored. The region of self-alignment is the largest of any of the voxel shapes (approximately $\frac{1}{2}$ the diameter). Passive alignment of spherical voxel layers is simple since rotation is irrelevant. However, an obvious drawback is the lack of geometric interlocking. This necessitates an additional post-processing step to bind the build materials and remove the sacrificial material, either mechanically, chemically, or thermally.

Spherical voxels are especially attractive as they are relatively easy to manufacture in bulk and are readily available for a large range of materials (steel, aluminum, copper, delrin, acrylic, etc.). Moreover, a number of techniques are available for fabricating high precision nanoscale spheres (Kawaguchi, 2000).

“GIKs”

There are also voxel designs which are exclusively non-space-filling, such as the Great Invention Kit (GIKs; Figure 4) being investigated by Popescu *et al.* (2006a). These are designed to geometrically interlock using simple 2D shapes, which are simple to fabricate. However, in order to interlock purely 2D shapes, an extra dimension of complexity must be incorporated into the assembly process.

Two-phase digital materials

Digital voxels may also consist of multiple subcomponents, allowing for simpler voxel fabrication and potentially richer design space at the expense of assembly effort. For example, all the basic 2D tessellating shapes presented in the 2.5D section can be kept as a strictly 2D layer and joined to adjacent layers with pin segments (Figure 5).

We performed qualitative analysis in the form of a weighted design matrix on these different voxel designs to summarize their strengths and weaknesses. They were evaluated on six different categories:

- 1 *Self-alignment.* How large is the region of self-alignment in comparison to the size of the voxel?
- 2 *Rotation/flip invariance.* How difficult is it to passively align a layer of voxels for placement?
- 3 *Interlocking.* Does the voxel physically interlock?
- 4 *Space filling.* How much of R^3 can the voxels fill?
- 5 *Manufacturability.* How easy is it to create millions of microscale voxels, based on current manufacturing technology?
- 6 *Assembly complexity.* How many dimensions/degrees of freedom are needed for an automated digital fabricator to assemble objects?

Subjective categories were evaluated on the basis of very poor (0), poor (2), satisfactory (5), good (8), and very good (10). Weights for each category were chosen according to our intuition of how important each aspect will be in creating a useful digital fabricator. Spherical voxels had the highest utility (Table I), because of their ease of assembly, manufacturability, and infinite rotation and flip invariance. Square and hexagon tile-based designs are the most promising of the space filling designs because they can be manufactured easily using existing multilayer fabrication processes and can easily be assembled layer by layer.

Analysis of digital materials

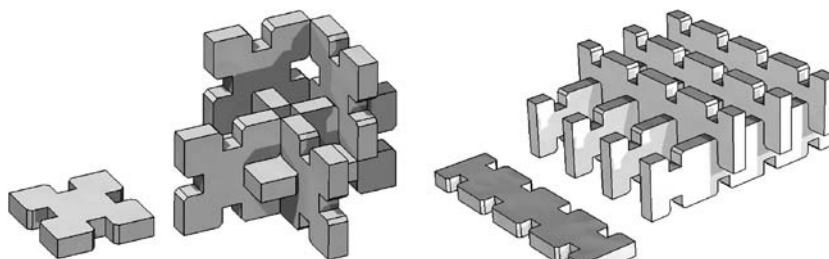
Of the voxel designs presented above, two of the most promising designs (highest utility) for a massively parallel assembly process were selected for detailed analysis. Because the voxels self-align upon being assembled, the overall assembly accuracy of digital material is determined solely by the precision of the individual voxels, not by the fabrication process. Thus, it is necessary to determine how the error of the overall structure scales with respect to manufacturing errors in the individual voxels.

Sphere analysis

First, we derive the theoretical basis for how error scales using spherical voxels. Spheres are ideal because the interaction between voxels is simple and easily modeled. In this analysis, the random dimensional errors (Coble, 1973) are assumed to be small relative to the size of the spheres, such that they stay on a recognizable lattice and the angle of interaction between spheres changes insignificantly. In the 1D case (a line of spheres), the dimensional error can be calculated analytically. The mean and variance of a single uniform distribution are:

$$\mu = \frac{1}{2} \left(\left(d + \frac{\varepsilon}{2} \right) + \left(d - \frac{\varepsilon}{2} \right) \right) = d \quad \text{and} \quad \sigma^2 = \frac{1}{12} \varepsilon^2,$$

Figure 4 Sparse digital matter (GIKs)



Source: Popescu *et al.* (2006b)

Figure 5 Example of multi-phase digital material using square tiles

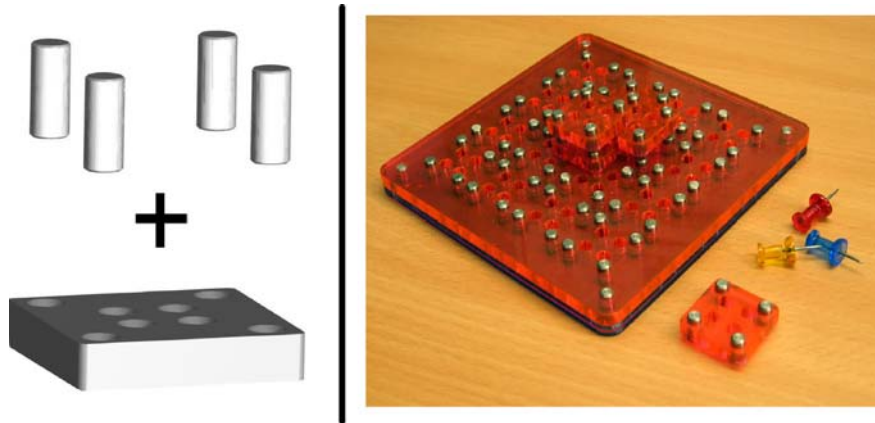


Table I Qualitative analysis shows that spherical and square-tile-based voxel designs are most suitable for a massively parallel top-down assembly process

Class	Base	Self-alignment (10)	Rotation/flip invariance (20)	Inter-locking (5)	Space filling		Assembly complexity (35)	Total (100)
					(5)	Manufactur-ability (25)		
2.5D	Diamond	Poor	Poor	Yes	> 95	Satisfactory	Poor	36
	Triangle	Poor	Satisfactory	Yes	100	Satisfactory	Satisfactory	52
	Square	Poor	Good	Yes	100	Good	Good	76
	Hexagon	Poor	Satisfactory	Yes	100	Good	Good	70
3D	Cube	Poor	Good	Yes	100	Poor	Poor	40
	Octahedra	Poor	Satisfactory	Yes	100	Poor	Very poor	27
	Tetrahedron	Poor	Satisfactory	Yes	100	Poor	Very poor	27
Spheres		Very good	Very good	No	79	Very good	Very good	94
GIKs		Good	Good	Yes	< 63	Very good	Poor	64
Multi-phase		Good	Good	Yes	100	Good	Poor	61

where d is the diameter of the spheres which varies uniformly within a given tolerance range ϵ . Given constant nominal diameters and tolerances, summing N uniform distributions results in:

$$\mu_N = N \times d \quad \text{and} \quad \sigma_N^2 = \frac{N}{12} \epsilon^2,$$

where μ_N and σ_N are the total mean and variation. Thus, stacking a 1D line of voxels gives a dimensional standard deviation of:

$$\sigma_{1D} = \epsilon \sqrt{\frac{(N - 0.5)}{12}} + c, \tag{1}$$

where σ_{1D} is the standard deviation of length ($N - 0.5$), is the effective number of voxel layers which (along with a small constant correction c) accounts for the physical constraints of the first voxel, and ϵ is the overall tolerance ($\pm \epsilon/2$) of each spherical voxel. For higher dimensions, a geometric lattice calculation yields:

$$\sigma_{2D} = \sqrt{\frac{3}{4}} \sigma_{1D} \quad \text{and} \quad \sigma_{3D} = \sqrt{\frac{2}{3}} \sigma_{1D}. \tag{2,3}$$

In the 2D case, spheres are assumed to be on a hexagonal grid. Patterning on a square grid would result in largely

decoupling the interactions between dimensions, so the 1D case would hold true in both dimensions. In the 3D case the spheres are in a hexagonal close-packed lattice structure. Other lattice structures would result slightly varying coefficients based on the difference of interaction angle between spheres in the third dimension. However, all these equations can be consolidated into a single worst-case equation when put in terms of the overall dimension L by multiplying the number of layers N by the normal distance between them. The resulting equation holds for all 3D if the number of spheres is large:

$$\sigma_L \approx \epsilon \sqrt{\frac{L}{12d}}. \tag{4}$$

We confirmed the standard deviation calculations for 1D, 2D, and 3D cases of spheres, and for square tiles in large-scale numerical simulation. A relaxation algorithm (Lipson, 2006) was run to settle each simulated structure under gravity. In the 1D and 2D cases this was carried out in Matlab, but the 3D case was implemented in C++ for superior speed. The vertical error of the topmost voxel from its nominal position was recorded and normalized by the tolerance range of the voxels. Voxels with nominal diameters of 1mm varying uniformly randomly within a given tolerance of 0.002mm were generated and stacked in a 1D vertical line or a 2D/3D

pyramid, yielding an ϵ/d ratio of 0.2 percent. This was repeated for voxels stacked to varying heights with 1,000 runs per height. The standard deviation of vertical positions for each height was output and plotted in Figure 6.

The data for the 1D and 2D cases confirm the analytical analysis. The 3D case illustrates increased error cancelling above ten voxels that was not included in the analytical analysis, and is fit more accurately with a lower exponent (cube root). This is because there are more paths for random errors to average out. This favorable property is not necessarily valid for structures that are thin relative to the size of the voxels. However, due to the limitations of layered manufacturing processes, a sacrificial material must be included in the printing process. These extra voxels (in the form of a stable pyramid) not only support the thin structure, but also impart their precision, effectively eliminating this issue. The implications of this for a practical sphere printer are good. For example, using $100\ \mu\text{m}$ spheres with tolerance $\epsilon = 5\ \mu\text{m}$

will allow fabrication of a 10 cm-scale 3D part with $100\ \mu\text{m}$ resolution and dimensions with a $45\ \mu\text{m}$ standard deviation.

Tile analysis

Similarly, a 3D simulator was programmed for the square tile-based voxel design. Each tile was modeled as four separate points (Figure 7) connected rigidly. Both the dimensions of the tiles and the locations of the out-of-plane joints were varied uniformly within the tolerance range ϵ , representing the accuracy of the voxel manufacturing process. In the numerical simulation of the tiles, several assumptions were made. First, the tile errors were kept small relative to the size of the tiles. Thus, the ratio of the error ϵ to the tile size D (ϵ/D) was less than 1 percent. This allowed the small angle assumption to be made in calculating forces involved. Interactions with adjacent tiles in plane were modeled as a contact force (pushing, but no pulling), and X/Y interactions with the tiles directly above and below were modeled with a

Figure 6 Multi-dimensional digital structure precision

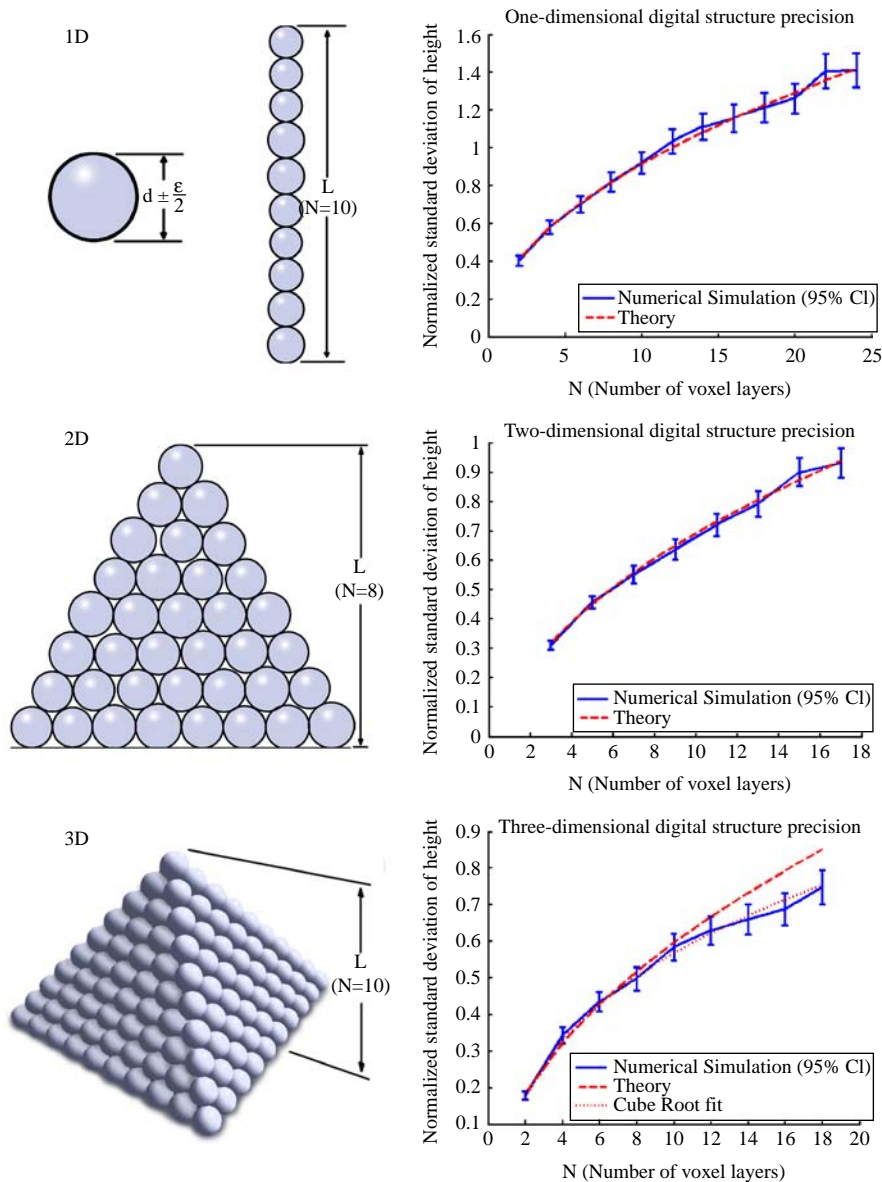
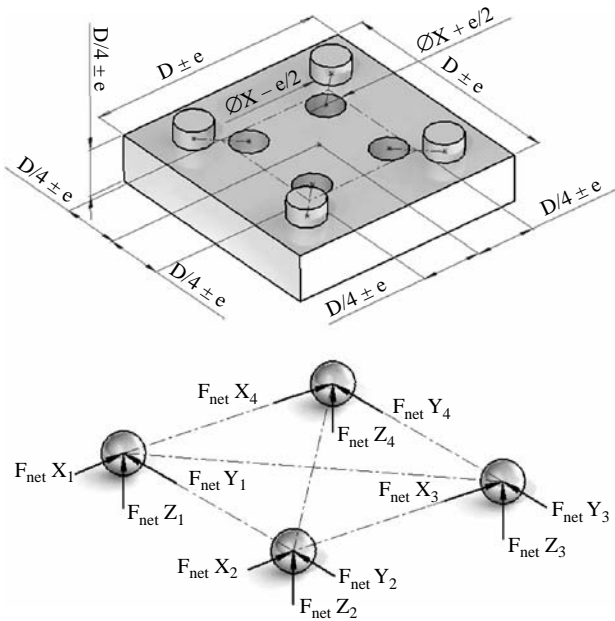


Figure 7 Dimensions, errors, and forces involved in large-scale tile numerical simulation



small dead zone around equilibrium to represent inaccuracies in the fit. This dead zone was sized such that based on the manufacturing tolerances of the tiles, the largest possible peg would always fit in the smallest possible hole.

Using the principle of relaxation, a simulator was implemented in C++ for quick multi-processor calculation (Figure 8). Cubes of simulated tile voxels were generated with dimensions $N \times N \times N$, filling the space between $(0,0,0)$ and $(N-1, N-1, N-1)$. Each tile was modeled with uniform random errors and the entire structure was relaxed. These structures were loosely constrained along the X, Y, and Z planes, and for each trial the location of the tile at (N,N,N) was recorded, representing the overall size of the digital-material cube. For each dimension of cube, 1,000 trials were completed to obtain good statistical significance. The standard deviation of these trials are plotted in Figure 9 with varying N. The optimized simulation ran for about 20h on four CPU cores simultaneously to obtain these results.

As observed with the spherical voxels, the error scales with a power law. In the X and Y dimensions, this exponent is much lower (about 0.1) than observed in the Z dimension and with

spherical voxels (exponent of about 0.5). Thus, if a multilayer lithography process can create 1mm tiles with a precision of $1 \mu\text{m}$, a one cubic meter ($1000 \times 1000 \times 1000$ units) structure would have dimensional error of less than $2 \mu\text{m}$ in the X and Y directions, and an error of about $30 \mu\text{m}$ in the Z direction.

Additional simulations were carried out to determine how the overall error of the structure varies with the error of the individual tiles over three orders of magnitude of errors. Cubes of tile voxel $10 \times 10 \times 10$ were generated and relaxed with unit tile size and voxel precisions ranging from 10^{-5} to 10^{-2} . For each precision level, 1,000 runs were completed and the standard deviation of voxel $(10,10,10)$ was recorded and normalized by the current voxel precision. As long as the error of the tiles is small (< 1 percent of the size), the relationship is direct (linear with a slope of 1; Figure 10). Thus, a voxel manufacturing process that improves precision by 50 percent will increase the precision of a digital structure by 50 percent.

Stress strain performance

Simulated stress/strain tests were conducted to determine how the macroscopic properties of digital materials change with the precision of the individual voxels. Structures of size $(10,5,10)$ were created, and a simple brittle material model was implemented for the tiles. This entailed a constant modulus of elasticity up to an ultimate stress, at which fracture occurred. Two trials were conducted, with high and low precision voxels ($\epsilon/D = 0.01$ and 1 percent, respectively). The structures were then incrementally elongated in the X direction and allowed to fully relax between increments, ensuring that the results are independent of the relaxation algorithm (Figure 11). The high precision tiles emulated the brittle material model of the individual tiles, with a very linear elastic modulus until fracture. With all other factors held constant, the low precision tiles displayed a notably ductile behavior. This included an “uptake” region of steadily increasing elastic modulus as the slack was taken up between tile interfaces, a linear region, a region of incremental failure as individual interfaces began to break, and lastly a region of cascading failure.

Extension to other voxel geometries

Based on the results of the sphere and square tile simulations, there are two classes of voxel interfaces that govern how error in a digital object scales: contact-only force transmission (voxels can only push against each other) and bi-directional force transmission (voxels can push or pull against each other). Contact only force (spheres, Z direction of tiles) scales roughly with the square root of the number of layers.

Figure 8 Screenshots from one relaxation iteration for a $10 \times 10 \times 20$ tile-voxel based structure. Yellow nodes with green force vectors represent unrelaxed areas, whereas red and blue links represent the residual tension and compression forces (respectively) within the tiles after relaxation

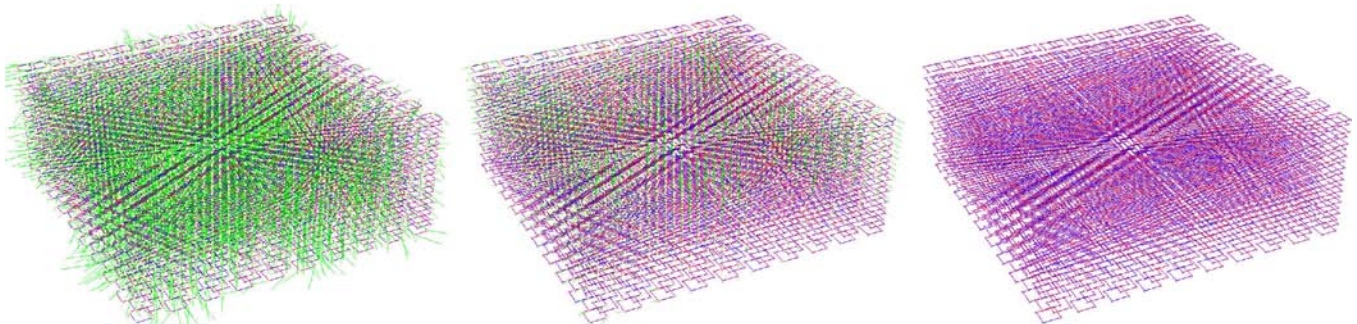


Figure 9 Digital structure precision for tile structures. Total error scales with a power law in respect to the size of the structure. In the X/Y direction, active force cancellation leads to a very low exponent ($x^{0.1}$), whereas in the Z direction, similar results to spheres are observed ($x^{0.5}$)

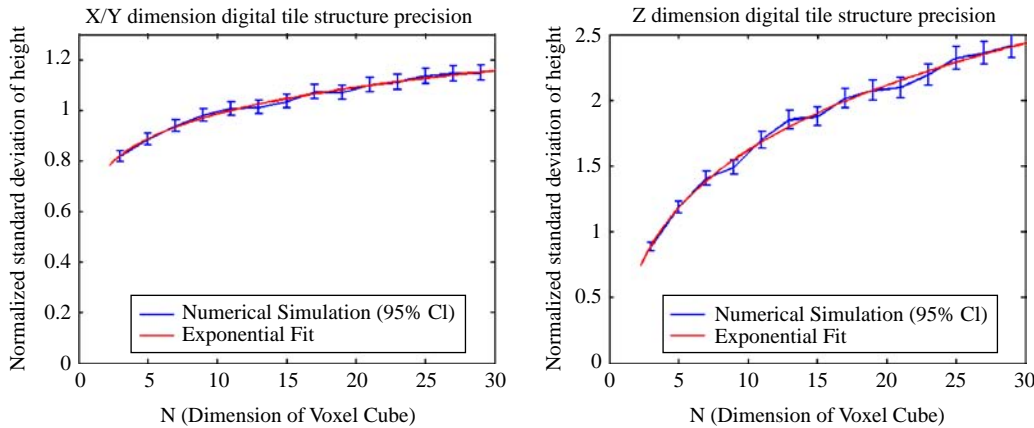


Figure 10 The precision of a digital structure varies directly with the precision of the tiles (ϵ)

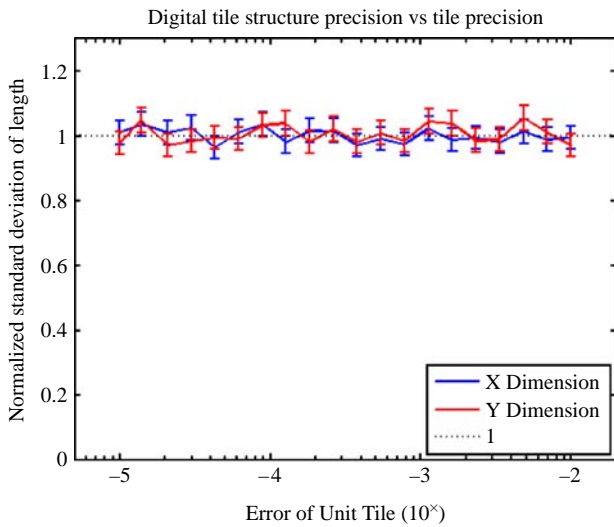
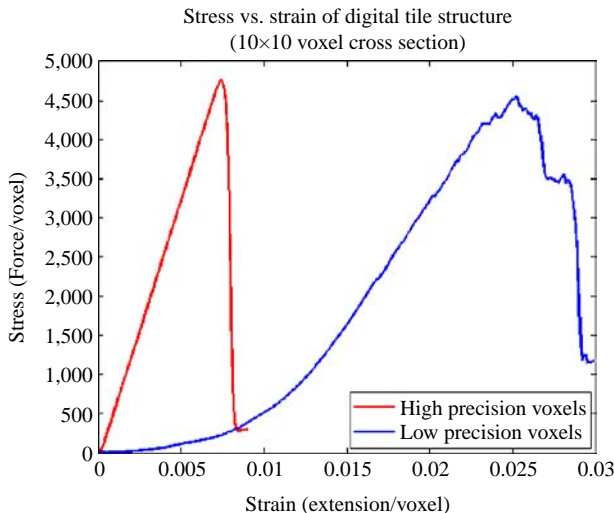


Figure 11 Stress/strain simulations of digital tile structures with varying precisions (ϵ) shows a transition from brittle to ductile behavior as the precision gets worse



Bidirectional force (X, Y direction of tiles) scales by a power law with the exponent being significantly less (0.1 in this simulation). Thus, it is possible make useful predictions regarding how error scales in any of the other voxel designs based on which interactions they experience.

Digital manufacturing technology

The process of transitioning from virtual voxels to physical voxels may be accomplished in several ways. The voxels may be fabricated in situ, using either inkjetting technology to deposit liquid droplets that subsequently harden, or a DLP system to selectively harden pixels within a layer of homogenous photo-curable material. In situ fabricated voxels are often quick and economical to work with, but they do not retain their digital (discrete) nature upon instantiation, are limited to very specific subsets of materials, and do not display the precision characteristics presented here. The prefabricated voxels used in physical 3D voxel printing, although requiring a more involved fabrication process, remain discrete and may be fabricated of any solid material.

The technology to create and assemble large-scale parts made of digital materials is in place and needs only to be reduced to practice. In order to specifically address any given voxel, the assembly process should be top down, as opposed to the bottom up approach used in self-assembly (Whitesides and Gryzbowski, 2002). The main technical hurdle is to deterministically assemble millions of voxels. In order to accomplish this in a reasonable amount of time, the assembly process itself must be massively parallel.

There are varying degrees of parallelism to assemble digital materials. A serial assembly process would place one voxel at a time. A 1D parallel process would place a line of voxels simultaneously, a 2D parallel process would place an entire layer, and a 3D parallel process would fabricate the entire digital part at once. Adding each dimension of parallelism results in vastly reduced assembly times as the process scales up to large numbers of voxels.

Since no technology is available for a 3D parallel assembly process, the most efficient approach will be a 2D parallel assembly process. When considering multiple materials, the time to assemble a cubic $l \times l \times l$ digital object for 1D and 2D parallel processes are:

$$t_{total,1D} = n \times t_{layer} \times l^2 \quad \text{and} \quad t_{total,2D} = n \times t_{layer} \times l,$$

where l is the number of voxels in each direction, n is the number of materials, and t_{layer} is the time needed to place a single arbitrary layer of voxels. This time would vary for the 1D and 2D assembly cases, but even if placing a layer takes twice as long as a line of voxels, a 2D parallel process is faster for $l > 2$. When $l = 100$ (a one mega-voxel printer), the 2D parallel process would be 50 times faster than a 1D parallel process.

In order to manipulate an arbitrary 2D array of voxels, an $l \times l$ printhead must be capable of attracting or repelling voxels at any of its l^2 locations. This requires individually addressable cells capable of producing a binary force (on or off). This force could be pneumatic, electrostatic, magnetic, surface tension, or any number of others. The minimum number of control lines to individually address of each cell scales favorably as l increases using multiplexing, but this requires a force that can be autonomously maintained in either the on or off state when not being addressed. This rapidly leads to scaling problems when l becomes large with the necessity of l^2 voxel holding cells. Thus, in order for 2D parallel assembly to scale up favorably, the voxel holding cells should themselves be capable of parallel fabrication.

The problem of individually addressing arbitrary locations within a large 2D matrix has been reduced to common technology with the advent of the personal computer. The output of a computer graphics card can address more than 20 million pixels at 16 bits and 60 Hz (Nvidia, 2007), which is more than sufficient to process 20 megapixel layers at once. Assuming a cubic build space, this is sufficient to enable an 80 Gigavoxel digital fabricator. The challenge is turning the digital output into physical forces to manipulate voxels. By coupling the computer output to a monitor or projector, the optical images can be used as an input for massively parallel manipulation of 2D fields (Chiou *et al.*, 2005). Optics can scale this output to any resolution and photosensitive components used to manage the forces. For instance, a photoconductive head material could be used in a process similar to laser printing, where each pixel picks up a distinct voxel instead of a dusting of toner. This exploits electrostatic forces, which are sufficient to deterministically manipulate parts at a sub-millimeter scale (Bohringer *et al.*, 1998). As voxel sizes become smaller, surface tension and Van der Waals forces also become far more significant than gravity (Fearing, 1995).

Sample structures

To illustrate the concept of a robust digital structure using spherical voxels, a 60 voxel cylinder and a 0.8 kilo-voxel sphere were assembled by hand using 1.5 mm (1/16 in.) spherical voxels (Figures 12 and 13). An "eggcrate" of wells was laser-cut to place the initial layer. For the cylinder, steel voxels were stacked layer by layer, surrounded by acrylic spheres as necessary to create a stable, self-aligned structure under gravity. Between each layer, a coating of aerosol spray adhesive (3M Super 77) was applied. The finished structure was removed from the base and placed in an oven at 260°C (500°F) for 30 min to melt away the acrylic and infuse the remaining voids in the steel structure. The finished part is robust and able to withstand repeated handling and dropping.

Hybrid bottom-up and top-down digital manufacturing

There is currently a dichotomy between top-down and bottom-up manufacturing: self-assembly is advantageous for fabricating simple, regular, small scale structures, but does not scale to complex (non-regular) macroscopic structures (Whitesides and Gryzbowski, 2002). Conversely, top-down manufacturing does not scale well to create complex nanoscale features. Digital fabrication offers the opportunity to bridge this gap by allowing nanoscale self-assembly to be used for massively parallel fabrication and alignment of relatively simple voxels, and then using top-down digital manufacturing to assemble complex macroscale structures out of the self-assembled voxels. For example, DNA self-assembly can be used to make spheres (Luo *et al.*, 1999) or cubes (Chen and Seeman, 1991), and other shapes (Liddell and Summers, 2003). These voxels, in turn, can be assembled in a top down way using a fabricator.

Potential applications of digital materials

The ability to assemble an arbitrary structure out of a large number of voxels is a powerful tool. Besides, fabricating complex and accurate geometries, in principle digital manufacturing allows for use of any material that is rigid at the time of assembly. It is here that digital manufacturing enables applications not possible with current RP/RM processes and introduces new possibilities to the MEMS community as well. Some specific examples follow:

- *Electrical networks.* Digital materials could be used to make extremely compact, integrated 3D electrical networks and microrobots. With a small library of conductive, insulating, transistor, and other electrical component voxels, compact custom 3D integrated circuits can be fabricated in one step – complete with fluidic cooling channels. By including piezo-electric or shape memory alloy voxels for sensing and actuation, all the components to create a robot in any form are in place, except power.
- *Fluidic networks.* A small library of voxels with microfluidic functionality could be developed to enable 3D integrated microfluidic circuits for chemical and biological uses. In fact, only two voxel types are needed to create arbitrary 3D fluidic networks (Figure 14). Compatible valving systems and sensing solutions would allow not only quick fabrication of 3D microfluidics, but eliminate the high overhead and the difficulty of aligning individual layers in traditional microfabrication labs.
- *Photonics.* Digital materials may also benefit those at the forefront of photonics research. Currently, there are many simulations of 3D optical circuits that would usher in a new era of computation, but there is no way to readily produce them (Lin *et al.*, 1998). In general, optical circuits are constructed by arbitrary regular placement of high and low optical index elements within a larger matrix (Vlasov *et al.*, 2002). Even now, voxels (order 1,000 μm) could be used to verify these properties with microwaves, and as the scale of voxels approaches the wavelength of visible light (order: 0.5 μm), digital manufacturing will provide unprecedented ability to create optical circuits (Figure 14).

Figure 12 A sample digital structure using spherical voxels. (1) Initial layer on egg-crate; (2) finished structure and support; (3) removing support; (4) finished product (Thumb tacks for scale)

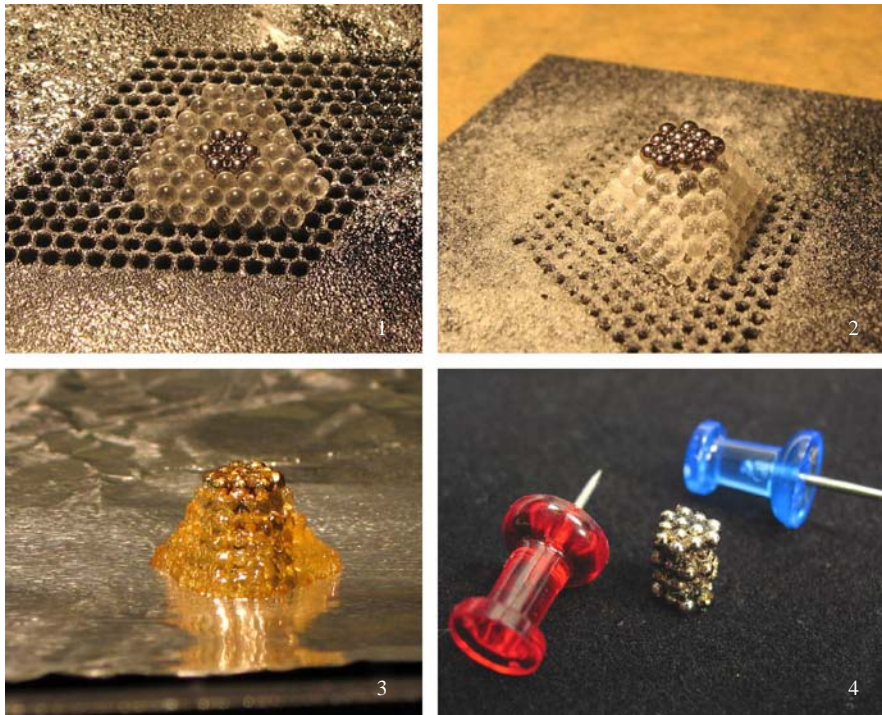


Figure 13 An 832 voxel sphere made of 1.5 mm steel spherical voxels and infiltrated with polyvinyl acetate glue



Future

We envision a standardized library of voxels that all have compatible geometry, in much the same way as TTL standardized the interface between digital circuit components in the 1960s. These voxels will be mass produced in high volumes, so that millions of voxels may be purchased for several dollars. Voxels would be manufactured several different ways, depending on the geometry, material

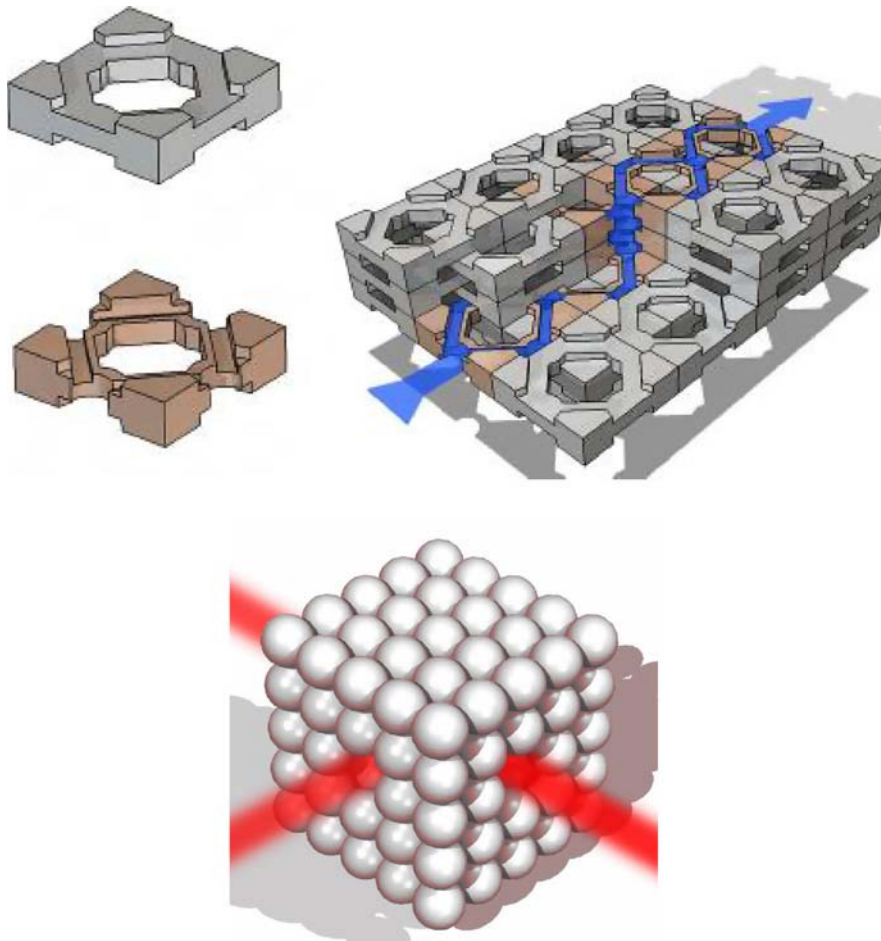
and size. For instance, 2.5D voxels such as those presented in Figure 2 may be produced at a microscale using multilayer photolithography techniques. Using a 300 mm wafer, a single wafer could produce more than 150 million 20 micron voxels. Producing microscale spheres of many different materials is also well understood, and a wide variety are commercially available. However, the voxel manufacturing techniques are highly specialized processes. Thus, it will be most economical to mass produce the voxels at central facilities. This concept of central manufacturing and distributed assembly is evident in products from LEGOs™ to modular structural components. As long as the function of each voxel is elementary, there will be a finite (and likely small) number of voxel types required to build arbitrarily complex objects.

The end-user would order voxels of many different materials and functions in disposable cartridges that are plugged into a digital fabricator sitting on a desktop. Then, plans for a glucose sensor, an educational microrobot, a portable music player, or any number of other products could be downloaded from the internet and fabricated at will.

Conclusions

Digital manufacturing exploits the accuracy of the building blocks rather than of the fabricator to achieve good precision, yet avoids the complexity barrier of traditional bottom-up self-assembly methods. The dimensional error of a macroscale digital object scales with only the square root of the number of microscale voxels for contact (pushing only) forces and much more favorably for interlocking tiles. Perfectly repeatable parts can be made, at the expense of a finite resolution and increased processing time.

Figure 14 Examples of advanced digital structures. Top: a square tile voxel used for printable arbitrary 3D microfluidic fluidic networks. Bottom: a photonic crystal



Several geometries are suitable for digital fabrication voxels, but with varying amounts of rotational symmetry that make passive alignment more simple. 3D interlocking blocks involve complex shapes that are hard to manufacture, but have 3D rotational symmetry. 2.5D blocks are simpler and easier to manufacture, but more likely to align in incorrect orientations. The biggest challenges of digital manufacturing involve processing large numbers of voxels quickly and accurately. Eventually, this technology will be expanded to include multiple useful materials that could be used for desktop fabrication of robots or other devices with integrated electrical or microfluidic circuits.

References

- Bohringer, K., Goldberg, K., Cohn, M., Howe, R. and Pisano, A. (1998), "Parallel microassembly with electrostatic force fields", paper presented at IEEE International Conference on Robotics and Automation (ICRA), Leuven, May.
- Calvert, P. (2001), "Inkjet printing for materials and devices", *Chemistry of Materials*, Vol. 13, pp. 3299-305.
- Chandru, V., Manohar, S. and Prakash, C.E. (1995), "Voxel-based modeling for layered manufacturing", *IEEE Computer Graphics and Applications*, Vol. 15, pp. 27-42.
- Chen, J. and Seeman, N. (1991), "Synthesis from DNA of a molecule with the connectivity of a cube", *Nature*, Vol. 350, pp. 631-3.
- Chiou, P., Ohta, A. and Wu, M. (2005), "Massively parallel manipulation of single cells and microparticles using optical images", *Nature*, Vol. 436 No. 7049, pp. 370-2.
- Chua, C.K., Chou, S.M. and Wong, T.S. (1998), "A study of the state-of-the-art RP technologies", *International Journal of Advanced Manufacturing Technology*, Vol. 14 No. 2, pp. 146-52.
- Chua, C.K., Leong, K.F. and Lim, C.S. (2003), *Rapid Prototyping: Principles and Applications*, 2nd ed., World Scientific, Singapore.
- Coble, R.L. (1973), "Effects of particle-size distribution in initial-stage sintering", *Journal of the American Ceramic Society*, Vol. 56, p. 461.
- Escher, M.C. (1971), *The Graphic Work of M.C. Escher*, Ballantine, New York, NY.
- Fearing, R.S. (1995), "Survey of sticking effects for micro parts handling", *Proceedings of the 1995 IEEE/RSJ International Conference on Intelligent Robots and Systems, IROS'95, Pittsburgh, PA*, Vol. 2, pp. 212-17.
- Gershenfeld, N. (2005), "Bits and atoms", *IS&T's NIP21: International Conference on Digital Printing Technologies, Baltimore, MD, September*, p. 2.

- Hollister, S.J. (2005), "Porous scaffold design for tissue engineering", *Nature Materials*, Vol. 4, pp. 518-24.
- Jense, G.J. (1989), "Voxel-based methods for CAD", *Computer Aided Design*, Vol. 21 No. 8, pp. 528-33.
- Kadekar, V., Fang, W. and Liou, F. (2004), "Deposition technologies for micromanufacturing: a review", *ASME Journal of Manufacturing Science and Engineering*, Vol. 126, pp. 787-95.
- Kawaguchi, H. (2000), "Functional polymer microspheres", *Progress in Polymer Science*, Vol. 25, pp. 1171-210.
- Liddell, C. and Summers, C. (2003), "Monodispersed ZnS dimers, trimers, and tetramers for lower symmetry photonic crystal lattices", *Advanced Materials*, Vol. 15 No. 20, pp. 1715-19.
- Lin, F. and Seah, H.S. (1998), "An effective 3D seed fill algorithm", *Computers & Graphics*, Vol. 22 No. 5, pp. 641-4.
- Lin, F., Seah, H.S., Wu, Z.K. and Ma, D. (2007), "Voxelisation and fabrication of freeform models", *Virtual and Physical Prototyping*, Vol. 2 No. 2, pp. 65-73.
- Lin, S.Y., Fleming, J.G., Hetherington, D.L., Smith, B.K., Zubrzycki, W., Kurtz, S.R., Bur, J., Biswas, R., Ho, K.M. and Sigalas, M.M. (1998), "A three-dimensional photonic crystal operating at infrared wavelengths", *Nature*, Vol. 394 No. 6690, pp. 251-3.
- Lipson, H. (2006), "A relaxation method for simulating the kinematics of compound nonlinear mechanisms", *ASME Journal of Mechanical Design*, Vol. 128 No. 4, pp. 719-28.
- Luo, D., Woodrow-Mumford, K., Belcheva, N. and Saltzman, W.M. (1999), "Controlled DNA delivery systems", *Pharmaceutical Research*, Vol. 16 No. 8, pp. 1300-9.
- Ma, D., Lin, F. and Chua, C.K. (2001a), "Rapid prototyping applications in medicine, part 1: NURBS-based volume modeling", *International Journal of Advanced Manufacturing Technology*, Vol. 18 No. 2, pp. 103-17.
- Ma, D., Lin, F. and Chua, C.K. (2001b), "Rapid prototyping applications in medicine, part 2: STL generation through volume modeling and iso-surface extraction", *International Journal of Advanced Manufacturing Technology*, Vol. 18 No. 2, pp. 118-27.
- Malone, E. and Lipson, H. (2006), "Freeform fabrication of ionomeric polymer-metal composite actuators", *Rapid Prototyping Journal*, Vol. 12 No. 5, pp. 244-53.
- Malone, E., Rasa, K., Cohen, D.L., Isaacson, T., Lashley, H. and Lipson, H. (2004), "Freeform fabrication of 3D zinc-air batteries and functional electro-mechanical assemblies", *Rapid Prototyping Journal*, Vol. 10 No. 1, pp. 58-69.
- Meagher, D.J. (1982), "Geometric modeling using octree encoding", *Computer Graphics and Image Processing*, Vol. 19 No. 2, pp. 129-47.
- Mullen, L., Stamp, R., Brooks, W., Jones, E. and Sutcliffe, C.J. (2008), "Selective laser melting: a regular unit cell approach for the manufacture of porous titanium, bone in-growth constructs", *Journal of Biomedical Materials Research: Part B – Applied Biomaterials – JBMR-B-08-0188*.
- Nvidia (2007), "Nvidia Quadro FX family features", available at: www.nvidia.com
- Popescu, G., Gershenfeld, N. and Marhale, T. (2006a), "Digital materials for digital printing", paper presented at International Conference on Digital Fabrication Technologies, Denver, CO, September.
- Popescu, G., Kunzler, P. and Gershenfeld, N. (2006b), "Digital printing of digital materials", paper presented at International Conference on Digital Fabrication Technologies, Denver, CO, September.
- Tolley, M., Zykov, V., Lipson, H. and Erickson, D. (2006), "Directed fluidic self-assembly of microscale tiles", *Proceedings of Micro-Total Analysis Systems (μ TAS), Tokyo, October*, pp. 1552-4.
- Vlasov, Y.A., Norris, D.J., Bo, X.Z. and Sturm, J.C. (2002), "On-chip assembly of silicon photonic band gap crystals", *Quantum Electronics and Laser Science Conference 2002 Proceedings*, pp. 116-17.
- Whitesides, G. and Gryzbowski, B. (2002), "Self assembly at all scales", *Science*, Vol. 295, March, pp. 2418-21.
- Yang, S., Leong, K., Du, Z. and Chua, C. (2001), "The design of scaffolds for use in tissue engineering. I. Traditional factors", *Tissue Engineering*, Vol. 7 No. 6, pp. 679-89.
- Yao, P., Schneider, G., Miao, B., Murakowski, J., Prather, D., Wetzel, E. and O'Brien, D. (2004), "Multilayer three-dimensional photolithography with traditional planar method", *Applied Physics Letters*, Vol. 85 No. 17, pp. 3920-2.
- Zhang, X., Jiang, X. and Sun, C. (1999), "Micro-stereolithography of polymeric and ceramic microstructures", *Sensors and Actuators A: Physical*, Vol. 77 No. 2, pp. 149-56.
- Zykov, V., Mytilinaios, E., Adams, B. and Lipson, H. (2005), "Self-reproducing machines", *Nature*, Vol. 435, pp. 163-4.

Further reading

- Gracias, D., Tien, J., Breen, T., Hsu, C. and Whitesides, G. (2000), "Forming electrical networks in three dimensions by self-assembly", *Science*, Vol. 289, pp. 1170-2.

Corresponding author

Jonathan Hiller can be contacted at: jdh74@cornell.edu